Journal of Magnetism and Magnetic Materials 465 (2018) 685–691

Contents lists available at ScienceDirect

Journal of Magnetism and Magnetic Materials

journal homepage: www.elsevier.com/locate/jmmm

Research articles

Theory of current-induced skyrmion dynamics close to a boundary

J.C. Martinez[a,*], W.S. Lew[b], W.L. Gan[b], M.B.A. Jalil[a]

[a] Computational Nanoelectronics and Nano-device Laboratory, National University of Singapore, 4 Engineering Drive 3, Singapore 117576, Singapore
[b] School of Physical and Mathematical Sciences, 21 Nanyang Link, Nanyang Technological University, Singapore 637371, Singapore

ARTICLE INFO

Keywords:
Skyrmion
Landau-Lifshitz-Gilbert equation
Thiele equation
Anisotropy

ABSTRACT

Skyrmions are the prime candidate as the information carrier of tomorrow's data storage devices. But they face the risk of annihilation on encountering a boundary. We show how skyrmions can avoid this undesired outcome through management of their anisotropy energies. Specifically we derive an edge potential and a contact interaction term which only operate close to the edge. We verify the accuracy of these two terms by modelling a realistic skyrmion system and comparing it with micromagnetic simulations. We not only observe and explain the speeding up of skyrmions near the edge (which had been expected) but also observe and explain a peculiar asymmetry in the motion (where it speeds up more on one edge compared to the other). We devise a means to stabilize a skyrmion against Magnus force (without the need for a transverse current) by modifying the damping parameters. Finally, we note a link between these damping parameters and the anisotropy energy. Our results will be of value in the design of skyrmion-based devices and would give fresh impetus to the study of magnetic anisotropy.

Significance: Skyrmions are the prime candidate as information carrier of tomorrow's ever ubiquitous data storage devices. But they face the risk of annihilation on encountering a boundary. We propose a model for the skyrmion-edge dynamics by deriving an edge potential and a contact interaction, which are incorporated into the standard Thiele equation for the current-induced motion of skyrmions. We compare this model with micromagnetic simulations which leads us to observe and explain the speeding up of skyrmions near the edge. We also observe and explain a peculiar asymmetry in the motion (where skyrmions speed up more on one edge compared to the other) and discover the important role played by the damping constants of the Thiele equation. We devised a means to stabilize a skyrmion against Magnus force (without the need for a transverse current) by modifying the damping parameters. A connection with the anisotropy energy is noted.

1. Introduction

Today's appetite for data and memory-device applications is being largely quenched by spintronics-research findings from over the past three decades, with current-induced phenomena in ferromagnets playing a leading role. Within this arena, attention has recently shifted onto the role of magnetic skyrmions in chiral helimagnets as information carriers [1]. Real devices are usually modelled upon planar geometries without boundaries but it is becoming increasing clear that boundary effects are not mere perturbations or harmless artefacts [2,3]. In fact the fate of skyrmions encountering a boundary is annihilation. We show in this paper that skyrmions can move even faster along a finite channel [4,5] and discuss how to optimize this circumstance. Thus what is new in this work is the management of the edge dynamics *in conjunction with* anisotropy engineering for the efficient control of skyrmion transport close to the track edge. These findings will be useful in the design and utilization of skyrmion-based devices and would also stimulate further studies in magnetic anisotropy.

Magnetic skyrmions are stable nano-sized vortex-swirls in non-centrosymmetric crystals harbouring great promise as information carriers and can be induced to motion under extremely low spin current densities [6–8]. For reviews see Refs. [9,10]. They have been created recently at room temperature and a demonstration of the controlled writing and deleting of skyrmions by spin-current injection has been lately achieved [11–13]. Skyrmions are produced in chiral magnets in the presence of the Dzyaloshinkii-Moriya interaction (DMI) which is also responsible in part for their remarkable stability [14]. In the past two years, skyrmions stabilized without or only partially by the DMI have been discussed and proposed as information carriers in the context of frustrated magnets in nanostrips [12,14–17]. We will not focus on these systems here.

Many applications of skyrmions as information carriers will require them to move on a track. An acute problem already noted above is their tendency to migrate toward an edge or boundary and annihilate there

* Corresponding author.
E-mail address: avecrux5@gmail.com (J.C. Martinez).

https://doi.org/10.1016/j.jmmm.2018.06.031
Received 21 November 2017; Received in revised form 1 June 2018; Accepted 11 June 2018

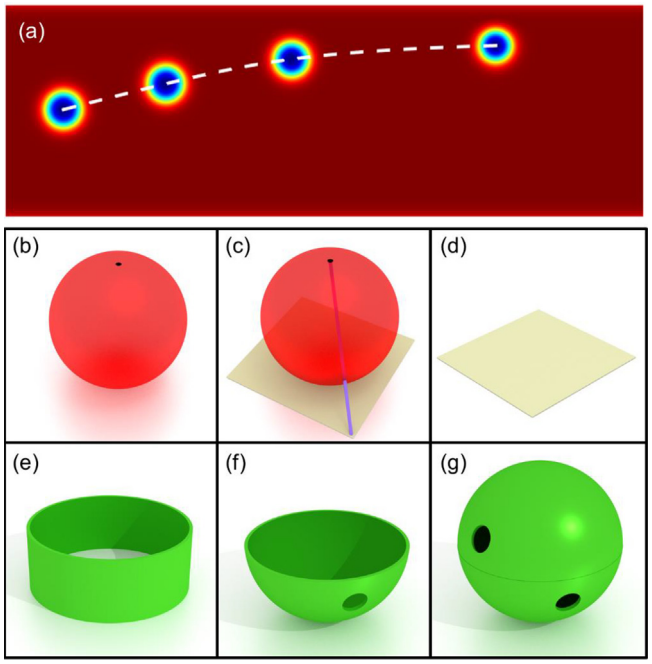

Fig. 1. Skyrmion trajectory and topology of an infinite plane and a finite channel: (a) Skyrmion trajectory on a finite track under a forward current to the right. The trajectory is generated from micromagnetic simulations which records positions at 0, 2, 4, 6 ns (see MethodsX, Section D). Note a drift upward caused by the Magnus force which ultimately pushes the skyrmion to the upper edge where it loses its topological protection and annihilates. (b) A plane is topological equivalent to a sphere with its North pole removed as shown by the homeomorphism between these surfaces via a stereographic projection from the North Pole (c) and (d). Similarly a finite track can be rolled into a cylinder (e) which in turn is homeomorphic to a hemisphere with a hole (f) or to a sphere with two points deleted (g). Thus a finite channel is topological distinct from a plane.

since they lose their topological protection at the edge. This is because of the Magnus force whereby current-induced motion is accompanied by a strong sideways force [19,20]. See Fig. 1(a). Skyrmions might avoid wandering by an edge if thermally induced magnons are able to cancel out the Magnus displacement [21]. However this scheme appears more complicated than the original system. Another way is for two perpendicularly magnetized ferromagnetic sublayers to couple antiferromagnetically with a heavy-metal layer beneath [22]. Skyrmion pairs of opposite vorticity are simultaneously created in the top and bottom layers and the pairs are capable of suppressing the Magnus displacement. Still another possibility is the use of a magnetic potential at the edges to confine skyrmions [23]. Despite their manifest merits, these all require *additional* elements integrated into the existing system.

In this paper we leave the track as is, but take advantage of the properties of the track edge, suitably re-engineering its anisotropy energies, so that annihilation is avoided *and* the skyrmions close to the edge are boosted forward faster those in the vicinity of the centre. We will also see that the spin-orbit interaction's role in the anisotropy energy is necessary in attaining these goals. A finite track is not infinite and a skyrmion is on the track only while it is traversing it and the skyrmion-migration problem is gone once the track is cleared.

Because our focus here is on skyrmion transport on finite tracks, it is important to establish early on the fundamental difference between finite and infinite tracks. Unlike the latter any finite track is not translationally invariant. Translation invariance is invoked to argue that skyrmions only experience the Magnus force, the dissipative force and whatever potential forces are present [18]. But this may be lost near an edge where left and right no longer pair. For any point on an infinite plane, a force from its left will be balanced by another from the right. Elements present in the plane may disappear in the finite channel and vice versa. Fig. 1(b–d) show how the plane is homeomorphic to a sphere with *one* point deleted, whereas a finite track is homeomorphic to a sphere with *two* points deleted (Fig. 1e–g). Moreover, we plot in Fig. 2 the configurations of the magnetization, the DMI and exchange fields on a track obtained from micromagnetic calculations; we see that the centre, whose environment resembles a plane, differs indeed from the environment of a point near an edge/boundary: the thinner the channel the greater that difference. Clearly the centre and edge environments are not merely different but fundamentally inequivalent: the axis-symmetry at the centre gives way to quasi-one-dimensional dynamics in the direction perpendicular to the edge.

In Section 2 we propose an analytical model for the skyrmion-edge dynamics by deriving expressions for the edge potential and contact interaction. These are two special features that figure when skyrmions are close to an edge. These are then incorporated into the standard Thiele equation for the current-induced motion of skyrmions in a finite channel. Armed with these tools we compare in Section 3.1 the model with micromagnetic simulations which leads us to observe and explain the speeding up of skyrmions near the edge. We also observe and explain a peculiar asymmetry in the motion (where skyrmions speed up more on one edge compared to the other) and discover the important role played by the damping constants of the Thiele equation in skyrmion transport. We devised in Section 3.2 a means to stabilize a skyrmion against Magnus force (without the need for a transverse current) by modifying the damping parameters. Finally in Section 3.3 we suggest future prospects and end with our conclusions.

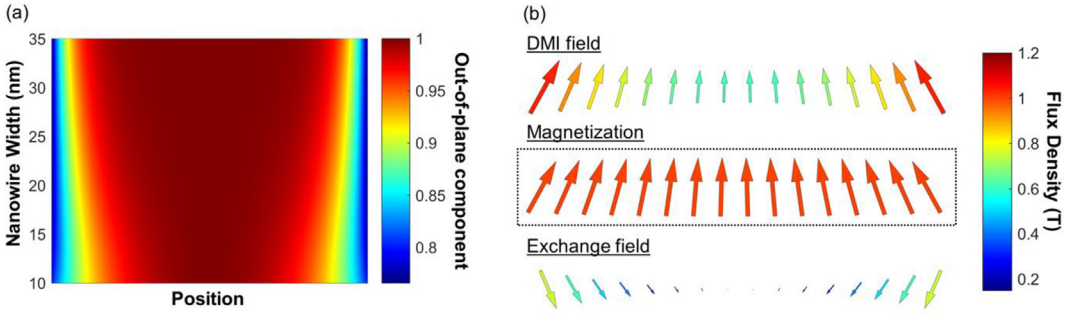

Fig. 2. Plots of the magnetization, exchange and DMI fields for a channel: (a) Variation of the out-of-plane magnetization across a finite width channel in a relaxed state versus position X in the channel, obtained from micromagnetic simulation (with periodic boundary conditions along X). The channel width (horizontal direction) is scaled to unity for any width. Colour gives the value of the reduced magnetization while the vertical axis gives the channel width. As noted in the MethodsX Section D, simulations should be for channel widths greater than 10 nm to be reliable. (b) Variation of the DMI (top) and exchange (bottom) fields across a 15 nm wide channel. The presence of growing fields close to the edge induces chiral twists. At the centre the magnetization is axisymmetric while at the edge it can be expected to display one-dimensional features in the direction perpendicular to the edge. These plots support the same conclusion in Fig. 1 that the plane and channel have fundamentally distinct physical environments.

2. Framework

2.1. Confined skyrmion system

We begin with the standard Landau-Ginzburg free energy for the *unconfined* skyrmion system, cast in terms of the local magnetic moment M treated as a classical vector of *fixed* length (due to translation invariance),

$$F_{\mathrm{LG}}[\boldsymbol{M}] = a\boldsymbol{M}^2 + J(\nabla \boldsymbol{M})^2 - D\left[(\hat{\mathbf{y}}\times\hat{\mathbf{z}})\cdot\left(\boldsymbol{M}\times\frac{\partial \boldsymbol{M}}{\partial y}\right) - (\hat{\mathbf{x}}\times\hat{\mathbf{z}})\cdot\left(\boldsymbol{M}\times\frac{\partial \boldsymbol{M}}{\partial x}\right)\right] + U\boldsymbol{M}^4 - \boldsymbol{B}\cdot\boldsymbol{M} \tag{1}$$

$J > 0$ is the exchange coupling, and a and U are anisotropy couplings [24,25]. The interfacial DMI with coefficient D arises from lack of inversion symmetry in chiral magnets [26] . The last or Zeeman term is from an external vertical magnetic field B. Above a transition temperature T_h the system is paramagnetic; below T_h and for a range of B, the skyrmion phase appears. This is implemented by taking a to be negative below T_{ch} and positive above, i.e., $a \propto (T - T_h)$.

Eq. (1) describes well an effective continuum theory for an *infinite* planar skyrmion system. Now near an edge it requires modification [27]. This was already implied at the end of Section I. In our context, we are interested in the dynamics of skyrmions *among* themselves (not on the structure of the skyrmion) in the *neighbourhood* of an edge/boundary (assumed straight for simplicity). Moreover **M** is *not* constant near the edge since there we lose translation invariance. The dynamics of skyrmions close to an edge has been studied lately [2,28,29] where the question of translation invariance is not taken up from the beginning. One of our main results, namely, the velocity enhancement close to the edge, has also been noticed before but not in the broader context of edge dynamics [30,31]. The role of magnons at the edge is not discussed here but was studied recently [32].

Before proceeding we highlight notions about stationary skyrmions that are implicit in this work. Micromagnetic simulations bear out these observations regarding inter-skyrmion interactions as well as their interaction with edges which we summarize in Fig. 3. There is *no* current to begin with; we are interested in the dynamics of stationary skyrmions within the channel. First, a skyrmion at the middle will remain there or slowly move about (Fig. 3(a)). Close to an edge a skyrmion will tend toward the interior (Fig. 3(b)). Two skyrmions positioned symmetrically at the centre will move apart (Fig. 3(c)) [27] as a consequence of their dipolar repulsion. But the same pair, if close to the edge, will tend to the interior (Fig. 3(d)). We conclude that the edge would repel a skyrmion toward the interior (Fig. 3(e)).

Unlike Eq. (1), the theory we seek is one-dimensional, perpendicular to the edge (taken as the y-direction, while the edge/boundary is in the x-direction). Hence at the edge we employ, instead of Eq. (1), the following free energy

$$F[m] = \int d^3x \left\{\frac{1}{2}r_0 M^2 + \frac{1}{2}\frac{J}{a_0}(\nabla M)^2 + \frac{1}{4}UM^4\right\} \tag{2}$$

where $J > 0$ also occurred above and constants r_0, and $U > 0$ are anisotropy parameters, $a_0$is the lattice spacing and $\boldsymbol{M}^2$is regarded as a particle density. Close to T_h, $r_0(T) \propto (T - T_h)$ with a positive pre-factor. Furthermore we interpret Eq. (2) to be the free energy for the normal component of M [33], see also MethodX, Section A.

In the above approximate picture we observe the notable absence of the DMI in Eq. (2). We know that in a one-dimensional theory at an edge, it can be absent from the field equation (see Section A of our MethodsX). Although the DMI has a role to play (e.g., shaping the skyrmion's helicity and furnishing a length scale [2]) it is not crucially influential in the dynamics at the edge (i.e., the inter-particle interaction at the edge which is our focus [15–18]). The DMI can be indirectly included through the boundary condition at the edge [27], but this is not required for our goal, namely, the transport problem (Section 2.2). Unlike Eq. (1), $F[m]$ describes a boson system (i.e., skyrmions) interacting via a quadratic and a quartic interaction. In the MethodsX section (Eq. (6)) we show that the solution of the field equation for $F[m]$ for $T < Th$ is (M is replaced by its normal component φ)

$$\varphi(y) = \pm\sqrt{\frac{|r_0|}{U}}\tanh\sqrt{|r_0|\,\frac{a_0}{2J}}\,(y - y_0) \tag{3}$$

y_0 being an arbitrary position near the edge (which can be determined by an edge boundary condition) and $U|\varphi|^2$ is the mean-field potential, $U = \frac{4\pi\hbar^2 a_s}{m}$, m the skyrmion mass and a_s the s-wave scattering length (positive for repulsive interactions) for binary collisions. This is the origin of the edge contact interaction (see Eq. (4) below). Estimates of the skyrmion radius and mass are $\frac{Ua_0}{8\pi J}$ 20 nm and 1×10^{-26} kg, respectively. (See MX, Section A.)

On account of solution (3) there is a one-dimensional potential close to the edge (see also MX, Eq. (6))

$$V_{\mathrm{edge}}(y) = \frac{1}{4}\frac{|r_0|^2}{U}\mathrm{sech}^4\sqrt{|r_0|\,\frac{a_0}{2J}}\,(y - y_0) \tag{4}$$

y_0 being where $V_{\mathrm{edge}}(y)$ peaks [2]. This is the *edge potential*. It is not of dipolar origin and is due to the interaction of skyrmions at the edge among themselves, i.e. collisions; ultimately it can be traced to the anisotropy energy (Section MX, Section A for discussion and references). A skyrmion approaching y_0 from the *interior* experiences a repulsion but on clearing this point it experiences a push toward annihilation. It is convenient then to exploit the repulsive part to retain skyrmions within the channel. Given the linear dependence of r_0 on $T - T_h$ we can choose an operating temperature T to optimize the strength of $V_{\mathrm{edge}}(y)$. For the edge potential we take $V_0 \equiv \frac{1}{4}\frac{|r_0|^2}{U}$ 300 ms^{-1}

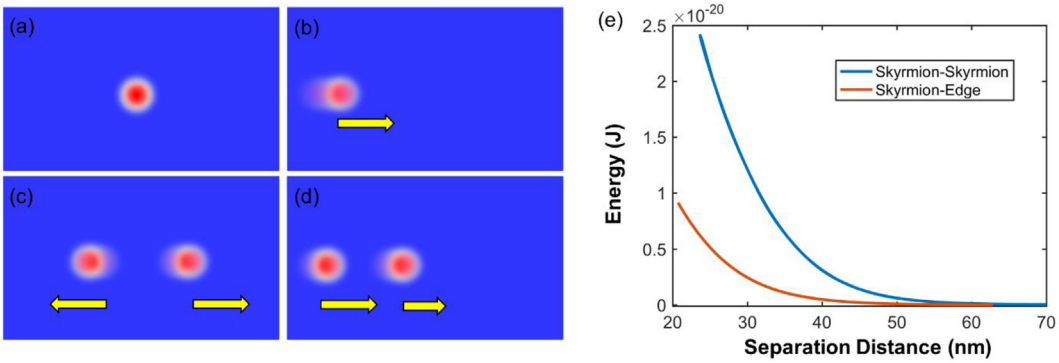

Fig. 3. Micromagnetic simulations of stationary skyrmions in a channel *without* driving current: (a) A skyrmion positioned at the centre will stay there; (b) if the skyrmion is close to the edge, it will move toward the interior; (c) two skyrmions at the centre will repel each other; (d) if the pair are close to the edge, both will tend toward the interior. (e) Repulsive energies on a skyrmion close to the edge and between two skyrmions at the centre of the channel.

and $\xi \equiv \sqrt{|r_0|\,\frac{a_0}{2J}} \approx 0.4\,\mathrm{nm}^{-1}$.

2.2. Skyrmion transport

To deal with skyrmion transport on a track, the standard Landau-Lifshitz-Gilbert (LLG) equation at $T = 0$ is usually invoked

$$\left(\frac{d}{dt} + (\mathbf{v_s}\cdot\nabla)\right)\mathbf{M} = -\gamma \mathbf{M}\times\mathbf{B}^{\mathrm{eff}} + \frac{\alpha}{M}\mathbf{M}\times\left(\frac{d}{dt} + \frac{\beta}{\alpha}(\mathbf{v_s}\cdot\nabla)\right)\mathbf{M} \tag{5}$$

$\mathbf{B}^{\mathrm{eff}} = -\frac{\delta \mathscr{H}}{\delta \boldsymbol{M}}$ is the effective field [11], $\mathbf{v_s}$ the velocity of electrons which is parallel to the applied current, and $\gamma = \frac{g\,|e|}{2m_e c}$ the gyromagnetic ratio [34]. Two dimensionless damping constants occur: the Gilbert constant α (typically 0.1) and β (assumed to be 0.3), which encapsulates the coupling between spin-polarized current and magnetization of nonadiabatic origin [35,36].

Because Eq. (5) is quite opaque, we employ here the much simpler Thiele equation, a mapped version of the former onto the skyrmion's steady-state translation modes [35]:

$$\mathbf{G}\times(\mathbf{v}_s - \mathbf{v}_d) + \overleftrightarrow{\mathscr{D}}(\beta\mathbf{v}_s - \alpha\mathbf{v}_d) = -\nabla V, \tag{6}$$

$G_k = \varepsilon_{ijk}\int d^2r \frac{1}{M^3}\mathbf{M}\cdot\partial_i\mathbf{M}\times\partial_j\mathbf{M}$ is the gyro-coupling vector, which is proportional to the topological winding number $W = -1$ per unit cell, $\mathbf{G} = 4\pi W\hat{\mathbf{n}}$ ($\hat{\mathbf{n}}$ being the unit normal) and $\overleftrightarrow{\mathscr{D}}_{ij} = \frac{1}{2\pi}\int_{UC} d^2r \frac{1}{M^2}\partial_i\mathbf{M}\cdot\partial_j\mathbf{M}$ the dissipative dyadic [19]. The gyro-term harks back to the Berry phase and pushes a skyrmion perpendicularly to its motion. It is the Magnus force discussed above. It exerts a dominant influence on skyrmion drift. The dissipation term sums up the skyrmion's tendency toward regions of lower energy, and originates from damping and nonadiabatic effects. It is not a topological invariant and is taken to be $\overleftrightarrow{\mathscr{D}}_{ij} = \mathscr{D}\delta_{ij}$, $\mathscr{D} \cong 5.577\pi$; $\quad i, j = x, y$ [37]. We have included a potential term V, which models a pinning or external potential. At the edge, we already saw the appearance of an *edge potential* $V_{\mathrm{edge}}(\boldsymbol{x})$ (see Eq. (4)). *Another* edge effect originates from the fact that the edge is a different environment from the center of the track, as we discussed in Section 1 and early in this section. Thus, near an edge we invoke the following form of the Thiele equation

$$\mathbf{G}\times(\mathbf{v}_s - \mathbf{v}_d) + \overleftrightarrow{\mathscr{D}}(\beta\mathbf{v}_s - \alpha\mathbf{v}_d) = -\nabla V_{\mathrm{edge}} - \int_{UC} d^2r \frac{1}{M}\partial_i\mathbf{M}\cdot\frac{1}{\hbar}\frac{\delta\mathscr{H}}{\delta\mathbf{M}} \tag{7}$$

which involves V_{edge} and the last term. This last term vanishes for an infinite plane because $\frac{1}{\hbar}\frac{\delta\mathscr{H}}{\delta\mathbf{M}} = 0$ in that case, but is non-vanishing at an edge. It is this term which distinguishes the finite channel from the infinite plane. We call it the contact interaction C (distinct from $V_{\mathrm{edge}}(\boldsymbol{x})$ of Eq. (4)) since it originates from contact between the skyrmion and the edge:

$$C \equiv -\int_{UC} d^2r \frac{1}{M}\partial_i\mathbf{M}\cdot\left(\frac{\partial\mathscr{H}}{\partial M}\right) \tag{8}$$

We solve for the skyrmion drift velocity $\boldsymbol{v}_{\mathrm{d}}$ from Eq. (6) for a channel (see Fig. 4 for geometry) and close to the edge where C and $V_{\mathrm{edge}}(\boldsymbol{x})$ operate:

$$v_{dx} = \frac{(G^2 + \alpha\beta\mathscr{D}^2)v_{sx} + G\mathscr{D}(\beta-\alpha)v_{sy} + \{G\partial_y V_{\mathrm{edge}}(\boldsymbol{x}) + \alpha\mathscr{D}\partial_x V_{\mathrm{edge}}(\boldsymbol{x}) - GC\}}{G^2 + \alpha^2\mathscr{D}^2} \tag{9}$$

$$v_{dy} = \frac{(G^2 + \alpha\beta\mathscr{D}^2)v_{sy} - G\mathscr{D}(\beta-\alpha)v_{sx} + \{-G\partial_x V_{\mathrm{edge}}(\boldsymbol{x}) + \alpha\mathscr{D}\partial_y V_{\mathrm{edge}}(\boldsymbol{x}) - \alpha\mathscr{D}C\}}{G^2 + \alpha^2\mathscr{D}^2} \tag{10}$$

We described $V_{\mathrm{edge}}(\boldsymbol{x})$ earlier (see Eq. (4)). C is a vector in the y-direction, and is non-zero only when the skyrmion approaches the edge.

2.3. Contact interaction

We estimate the magnitude of the boundary contact interaction, Eq. (8),

$$C = -\int_{UC} d^2r \frac{1}{M}\partial_i\mathbf{M}\cdot\left(\frac{1}{4}\frac{U\partial M^4}{\hbar\partial\mathbf{M}}\right). \tag{11}$$

We are using the cubic anisotropy term. Working this out, , *where*, where L is the length along x-direction and y-integration is only over that half of the skyrmion in contact with its neighbour and generates the hard-core interaction (see also MX, Section A). Observe that the integral over the whole skyrmion is *not* zero because M^2here is symmetric about the origin. To obtain a numerical estimate we note that $U\mathbf{M}^4$ is of order $10^3\,\mathrm{J/m^3}$. The saturation magnetization is of typically $4\times10^4\,\mathrm{A\,m^{-1}}$ and using $L = 40\,\mathrm{nm}$ we find $ULM^3 \approx 10^{-9}\,\mathrm{T\,m}$. Multiplying by $\gamma \approx \frac{10^{12}\mathrm{rad}}{6\mathrm{T\ s}}$ (for the definition of γ see Eq. (5)) we obtain $C \;\; 160\,\mathrm{nm/ns}$. However this estimate ignores dependence on the magnetization direction and temperature effects. (This value fits with our simulations.) It is clear that C can be varied through the anisotropy energy, as is the case with parameters α and β.

Incidentally, if we apply Eq. (11) to the DMI we obtain $\int_{UC} d^2r \frac{1}{M}\partial_i\mathbf{M}\cdot\frac{\delta}{\delta\mathbf{M}}\left[(\hat{y}\times\hat{z})\cdot\left(M\times\frac{\partial M}{\partial y}\right) - (\hat{x}\times\hat{z})\cdot\left(M\times\frac{\partial M}{\partial x}\right)\right]$. In obtaining

$$= \int_{UC} d^2r \frac{1}{M}\partial_i\mathbf{M}\frac{\delta}{\delta\mathbf{M}}\left[\hat{y}\cdot\left(M\times\frac{\partial M}{\partial x}\right)\right] \equiv 0$$

this result we used the fact that only the derivative *across* the strip (i.e., x-direction) can be nonzero for a planar system. This result means that the DMI interaction does not lead to an edge contact force. However it may have an effect through a boundary condition which we do not consider in this article. At any rate, the DMI effect may possibly be of higher order.

3. Results

3.1. Skyrmion trajectories with compensating current

We now discuss results obtained from the Thiele equation. Fig. 4(a) presents trajectories for skyrmion motion on a finite channel. They originate from the centre, the top and the bottom of the channel. Each trajectory is independent of the others and exhibiting them in one graph facilitates comparison. We assume skyrmions of radius 20 nm. All have the same driving spin current and their trajectories are compared as though in a race. Since the Magnus force pushes skyrmions up, a downward *compensating spin current* $v_{sy}$is applied to keep them on a horizontal path. During its run a skyrmion might protrude slightly at the edge but does not annihilate. Although v_{sy}leads to a Magnus drift along x, it is small (10%) compared with that of C. We will see later how the Magnus displacement can be mitigated without v_{sy}. Our purpose here is to appreciate the effect of C.

Interestingly and unexpectedly an asymmetry occurs in the dynamics with respect to the edges. For the top trajectory the skyrmion speed is 10% larger than that at the centre while the skyrmion at the bottom is slower by 15%. Clearly motion on the top is favoured while motion on the bottom edge is not, if speed is our goal. The effects of the top and of the bottom are opposite: the top edge aids motion, whereas the bottom deters it. On reversing the spin current, the edges exchange roles.

The central skyrmion experiences neither C nor V_{edge} and serves as a reference. Its velocity $v_{dx}(t)$ is larger than the spin current velocity on account of v_{sy}. For the trajectories near the edges, C operates. The signs of C are *opposite* for the edges since C is always directed *toward* the centre, whichever the edge. C has the effect of working *against* the spin current at the bottom edge, whereas it works *for* the current at the top. The drift velocity $v_{dy}(t)$ decreases to almost zero due to $V_{\mathrm{edge}}(\boldsymbol{x})$. On the other hand the effect of $V_{\mathrm{edge}}(\boldsymbol{x})$ on $v_{dx}(t)$ is slight.

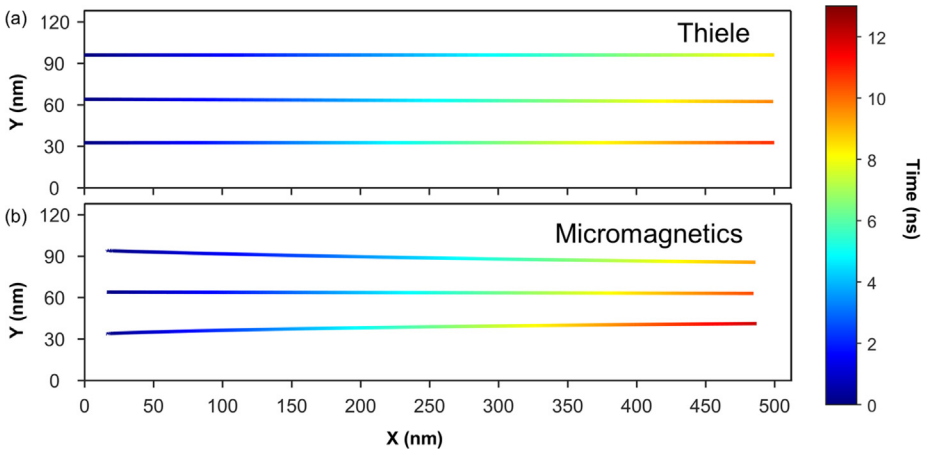

Fig. 4. Skyrmion trajectories along a channel 128 nm wide and 512 nm long. (a) Starting points are at the left edge $y = 34$ nm; centre $y = 64$ nm; and top edge $y = 94$ nm. All three have the same forward current velocity $v_{sx} = 50\,\mathrm{ms}^{-1}$. These are obtained using the Thiele equation. (b) The bottom panel is obtained from micromagnetic simulations with starting points: left edge $y = 34$ nm; centre $y = 64$ nm; and top edge $y = 94$ nm. In both cases the Magnus force is overcome by another spin current downward imparting an additional spin velocity component v_{sy} to the skyrmion (see MethodsX, Section C for more detail). Length and time are in nm and ns, respectively.

To understand the physics, we write Eq. (6) as $\mathbf{G}\times(\mathbf{v}_s-\mathbf{v}_d)+\overleftrightarrow{\mathscr{D}}(\beta\mathbf{v}_s-\alpha\mathbf{v}_d)=C\hat{y}$. For greater clarity in this task we omit for now the edge potential V_{edge}. This omission shows the conclusion more directly. The x-component is: $\frac{dv_{dx}}{dt}\approx v_{sx}+\frac{\mathscr{D}}{G}(\beta-\alpha)v_{sy}\pm\left|\frac{C}{G}\right|$, $\pm=\begin{matrix}\text{top}\\ \text{bottom}\end{matrix}$ which shows that C plays the role of a driving force in the x-direction. If we wish to see larger velocity enhancement we increase C. For results for other current velocities see MX, Section C. These latter results bear out the same conclusions given above and further reinforce them.

The analytical results above are also well corroborated by numerical simulations whose results are shown in Fig. 4(b). Specific details about these simulations have been relegated to the MX, Section D.

3.2. Skyrmion trajectories without compensating current

In Fig. 4 the Magnus force was compensated by a transverse current. To employ skyrmions in memory devices, it very useful to do away with this stratagem. We now turn to this goal and will see how V_{edge} plays an important role. From Fig. 5(a), we observe that v_{dy} decreases by setting v_{sy} to zero and allowing α to increase while β is simultaneously decreased. To mitigate the Magnus effect, it is not necessary for v_{dy} to vanish; it suffices that v_{dy} is small so that at the edge, V_{edge} stops the transverse drift. Guided by this insight, we set $v_{sy} = 0$ and choose $\alpha = 0.17$ and $\beta = 0.23$, keeping the same values for v_{sx}, V_0 and C. (This change in α and β will be attributed to the anisotropy; see below.) From these, we have $v_{dy} \sim -2\,\mathrm{ms}^{-1}$, at time $t = 2$ ns, which is small enough to be balanced by V_{edge}. The trajectory, shown in the multi-coloured track of Fig. 5(b), straightens toward the end due to V_{edge}. This becomes clearer with the other plot showing the transverse velocity v_{dy} against x. The transverse velocity $v_{dy} = -2\ \mathrm{ms}^{-1}$ at the start, drops to almost zero toward the end. V_{edge}, which is repulsive at some distance from the edge, caused this drop. The skyrmion keeps within the track and only at the end does its rim protrude slightly. The drift velocity $v_{dx} \approx 60\,\mathrm{ms}^{-1}$ and is increasing at the end reaching a value 20% higher than the spin current velocity. This is the edge-induced velocity enhancement mentioned above. With a suitable choice of α and β we can mitigate considerably the effect of the Magnus force and do away with a transverse spin velocity v_{sy} of the injected current (previously imposed in Fig. 4). Furthermore an additional advantage is an enhancement of the forward drift velocity. In MX, Section C, we give examples of velocity enhancement reaching 50%.

3.3. Beyond the Thiele equation

Fig. 6 shows trajectories from the centre of the track of Fig. 4, *but* without the compensating current $v_{sy}$and for $\alpha = 0.1$ and $\beta = 0.3$. These were obtained by micromagnetic simulation. Unlike Fig. 4, it is the forward current density J that is changing here. Two important observations are clear: (a) motion is accelerating as the skyrmions approach the edge; (b) the accelerations are current dependent and even decrease with current density. The first observation can be easily explained by the term $G\partial_y V_{\mathrm{edge}}(\boldsymbol{x})$in Eq. (8) (with y_0 at the edge), which shows that acceleration grows faster as the skyrmion nears the edge. Our analytical model does not capture some details about the edge. The second, however, is quite new and would possibly require amending the LLG equation. These point to future work; see also Ding et al. [38].

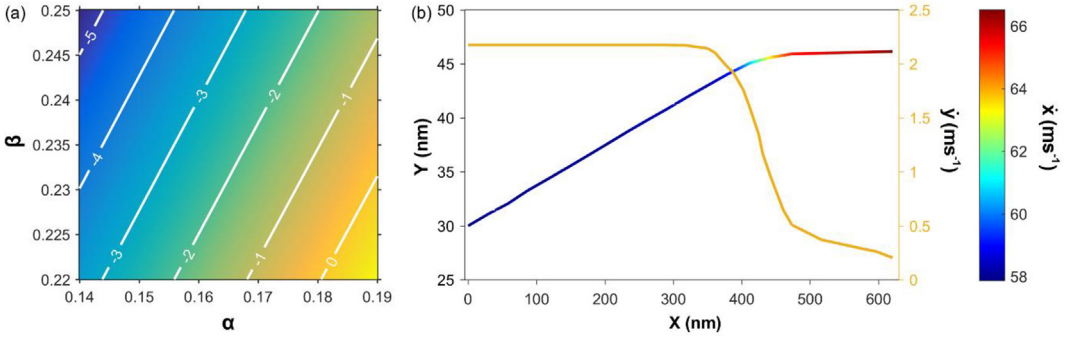

Fig. 5. Density plot of transverse drift velocity v_{dy} at time $t = 2$ ns and trajectory for zero transverse-spin-current: For both plots transverse spin velocity is $v_{sy} = 0$ while forward spin current $v_{sx} = 50\,\mathrm{ms}^{-1}$. (a) Horizontal and vertical axes give α and β respectively while colour gives drift velocity v_{dy}. This shows a trend toward smaller v_{dy} as α increases and β decreases from their initial values 0.1 and 0.3. (b) Skyrmion trajectory close to the top edge where colour gives the forward velocity v_{dx} (or $\dot{x}$). The second plot show x versus the transverse velocity v_{dy} (or $\dot{y}$). We chose $\alpha = 0.17$, $\beta = 0.23$ and set $v_{sy} = 0$. Note the effect of $V_{\mathrm{edge}}(x)$ in negating the transverse drift toward the end of the run. These results were obtained using the Thiele equations.

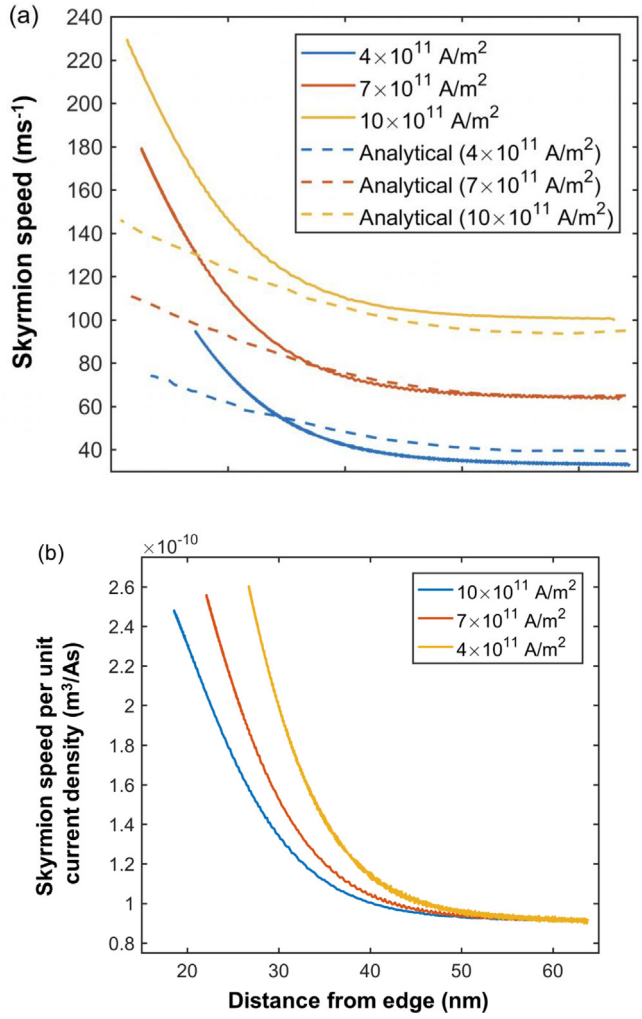

Fig. 6. Plots of the forward drift velocity v_{dx} versus separation from the edge for different spin currents. (a) The geometry is the same as Fig. 4. Here the vertical axis represents the forward skyrmion speed v_{dx} while the horizontal axis the separation from the edge. All skyrmions start at the centre. The Magnus force pushes all of them to the left. The plots show that the skyrmions are accelerating as they approach the edge and their acceleration is increasing monotonically. This can be understood from Eqs. (8) and (10) with y_0 = edge. (b) This is the same plot as (a) but the vertical axis now represents the velocity per unit driving current. It shows that the acceleration is current dependent but not in a linear fashion, implying some optimal current for skyrmion transport.

4. Conclusion

We sum up our results. After laying emphasis on the differences between skyrmion dynamics in the centre of a track and at the edges we proposed a one-dimensional theory of the interaction between skyrmions close to the edge in terms of a boson field theory with hard-core interaction. The contact interaction C at the edge translated into an edge force on skyrmions and, through the Magnus force, boosted them forward on the track. This additional force either speed up a skyrmion or slow it down depending which side the edge is. We verified this through micromagnetic simulations by comparing skyrmions moving on the left edge, centre and right edge of a track. This is the first time that an asymmetry in the motion of current-induced skyrmions has been reported and we also provided the underlying reason for it. We showed how the Magnus force, which pushes skymions off-track where they annihilate, can be weakened to mitigate this effect by varying the parameters α and β. This can be undertaking through suitable manipulation of the anisotropy energies. Thus the edge dynamics together with the management of the anisotropy energy can effect efficient and fast transport of skyrmions on a finite track. Another edge effect, V_{edge}, is weaker than the contact interaction but plays an assisting role in the dynamics.

Acknowledgments

We thank the MOE Tier II grant MOE2013-T2-2-125 (NUS Grant No. R-263-000-B10-112) and the National Research Foundation of Singapore under the CRP Programs “Next Generation Spin Torque Memories: From Fundamental Physics to Applications” NRF-CRP9-2013-01 and “Non-Volatile Magnetic Logic and Memory Integrated Circuit Devices” NRF-CRP9-2011-01, NRF-CRP9-2011-01 for financial support.

Appendix A. Supplementary data

Supplementary data associated with this article can be found, in the online version, at https://doi.org/10.1016/j.jmmm.2018.06.031.

References

[1] S. Krause, S. Wisendanger, Spintronics: skyrmionics gets hot, Nat. Mater. 15 (2016) 493–494.
[2] J. Iwasaki, M. Mochizuki, N. Nagaosa, Current-induced skyrmion dynamics in constricted geometries, Nat. Nanotechnol. 8 (2013) 742–747.
[3] J.V. Kim, F. Garcia-Sanchez, J. Sampaio, C. Moreau-Luchaire, V. Cros, A. Fert, Breathing modes of confined skyrmions in ultrathin magnetic dots, Phys. Rev. B 90 (2014) 064410.
[4] J. Iwasaki, W. Koshibae, N. Nagaosa, Colossal spin transfer torque effect on skyrmon along the edge, Nano Lett. 14 (2014) 4432–4437.
[5] W. Koshibae, Y. Kaneko, J. Iwasaki, M. Kawasaki, Y. Tokura, N. Nagaosa, Memory functions of magnetic skyrmions, J. Appl. Phys. 54 (2015) 053001.
[6] A. Fert, V. Cros, J. Sampaio, Skyrmions on the track, Nat. Nanotechnol. 8 (2013) 152–156.
[7] J. Sampaio, V. Cros, S. Rohart, A. Thiaville, A. Fert, Nucleation, stability and current-induced motion of isolated magnetic skyrmions in nanostructures, Nat. Nanotechnol. 8 (2013) 839–844.
[8] G. Finocchio, F. Büttner, R. Tomasello, M. Carpentieri, M. Kläui, Magnetic skyrmions: from fundamentals to applications, J. Phys. D: Appl. Phys. 49 (2016) 423001.
[9] Mochizuki Masahito, Current-driven dynamics of skyrmions, Topological Structures in Ferroic Materials, Springer International Publishing, 2016, pp. 55–81.
[10] N. Nagaosa, Y. Tokura, Topological properties and dynamics of magnetic skyrmions, Nat. Nanotechnol. 8 (2013) 899–911.
[11] N. Romming, C. Hanneken, M. Menzel, J.E. Bickel, B. Wolter, K. von Bergmann, A. Kubetzka, R. Wiesendanger, Writing and deleting single magnetic skyrmions, Science 341 (2013) 636–639.
[12] S. Woo, et al., Observation of room-temperature magnetic skyrmions and their current-driven dynamics in ultrathin metallic ferromagnets, Nat. Mater. 15 (2016) 501.
[13] Y. Tokunaga, X.Z. Yu, J.S. White, H.M. Ronnow, D. Morikawa, Y. Taguchi, Y. Tokura, A new class of chiral materials hosting magnetic skyrmions beyond room temperature, Nat. Commun. 67638 (2015), http://dx.doi.org/10.1038/ncomms8638.
[14] T. Kikuchi, T. Koretsune, R. Arita, G. Tatara, Dzyaloshinskii-Moriya Interaction as a consequence of a Doppler Shift due to spin-orbit-induced intrinsic spin current, Phys. Rev. Lett. 116 (2016) 247201.
[15] T. Okubo, S. Chung, H. Kawamura, Multiple-q states and the skyrmion lattice of the triangular-lattice Heisenberg antiferromagnet under magnetic fields, Phys. Rev. Lett. 108 (2012) 017206.
[16] A.O. Leonov, M. Mostovoy, Multiply periodic states and isolated skyrmions in an anisotropic frustrated magnet, Nat. Commun. 6 (2015) 8275.
[17] S. Hayami, S.-Z. Lin, C.D. Batista, Bubble and skyrmion crystals in frustrated magnets with easy-axis anisotropy, Phys. Rev. B 93 (2016) 184413.
[18] L. Rozsa, A. Deak, E. Simon, R. Yanes, L. Udvardi, L. Szunyogh, U. Nowak, Skyrmions with attractive interactions in an ultrathin magnetic field, Phys. Rev. Lett. 117 (2016) 157205.
[19] K. Everschor, M. Garst, R.A. Duine, A. Rosch, Current-induced rotational torques in the skyrmions lattice phase of chiral magnets, Phys. Rev. B 84 (2011) 064401.
[20] J.C. Martinez, M.B.A. Jalil, Topological dynamics and current-induced motion in a skyrmion lattice, New J. Phys. 18 (2016) 033008.
[21] S. Schroeter, M. Garst, Scattering of high-energy magnons off a magnetic skyrmion, Low Temp. Phys. 41 (2015) 817–825.
[22] X. Zhang, Y. Zhou, M. Ezawa, Magnetic bilayer-skyrmion without skyrmions Hall effect, Nat. Commun. 7 (2016) 10293, , http://dx.doi.org/10.1038/ncomms10293.
[23] I. Purnama, W.L. Gan, D.W. Wong, W.S. Lew, Guided current-induced skyrmion motion in a 1D potential well, Sci. Rep. 5 (2015) 10620.
[24] P. Bak, M. Høgh Jensen, Theory of helical magnetic structures and phase transitions

in MnSi and FeGe, J. Phys. C Solid. St. Phys. 13 (1980) L881-885m.
[25] Y. Ishikawa, K. Tajima, D. Bloch, M. Roth, Helical spin structure in manganese silicide MnSi, Solid State Commun. 19 (1976) 525–528.
[26] J.-H. Moon, S.-M. Seo, K.-J. Lee, K.-W. Kim, J. Ryu, H.-W. Lee, R.D. McMichael, M.D. Stiles, Spin-wave propagation in the presence of interfacial Dzyaloshinskii-Moriya interaction, Phys. Rev. B 88 (2013) 184404.
[27] S.A. Meynell, M.N. Wilson, H. Fritzsche, A.N. Bogdanov, T. Monchesky, Surface twist instabilities and skyrmion states in chiral ferromagnets, Phys. Rev. B 90 (2014) 014406.
[28] X. Zhang, G.P. Zhao, H. Fangohr, J. Ping Lin, W.X. Xia, J. Xia, F.J. Morvan, Sci. Rep. 5 (2015) 7643.
[29] S.-Z. Lin, C. Reichhardt, C. Batista, A. Saxena, Particle model for skyrmions in metallic chiral magnets: dynamics, pinning and creep, Phys. Rev. B 87 (2013) 214419.
[30] R. Tomasello, E. Martinez, R. Zivierri, L. Torres, M. Carpentieri, G. Finocchi, A strategy for the design of skymion race track, Sci. Rep. 4 (2014) 6784.
[31] J. Muller, A. Rosch, M. Garst, Edge instabilities and skyrmion creation in magnetic layers, N. J. Phys. 18 (2016) 65006.
[32] S. Zhang, Z. Li, Roles of nonequilibrium conduction electrons on magnetization dynamics of ferromagnets, Phys. Rev. Lett. 93 (2014) 127204.
[33] L.P. Pitaevskii, S. Stringari, Bose-Einstein Condensation, Clarendon Press, Oxford, 2003.
[34] A. Barman, S. Wang, S. Hellwig, A. Berger, E. Fullerton, H. Schmidt, Ultrafast magnetization dynamics in high perpendicular anisotropy [Co/Pt]n multilayers, J. Appl. Phys. 101 (2007) 09D102.
[35] O. Boulle, J. Kimling, P. Warnicke, M. Kläui, U. Rüdiger, G. Malinowski, H.J.M. Swagten, B. Koopmans, C. Ulysse, G. Faini, Nonadiabatic spin transfer torque in high anisotropy magnetic nanowires with narrow domain walls, Phys. Rev. Lett. 101 (2008) 216601.
[36] A.A. Thiele, Steady-state motion of magnetic domains, Phys. Rev. Lett. 30 (1973) 230–233.
[37] J. Iwasaki, M. Mochizuki, N. Nagaosa, Universal current-velocity relation of skyrmion motion in chiral magnets, Nat. Commun. 4 (2013) 1463.
[38] J. Ding, X. Yang, T. Zhu, Manipulating current induced motion of magnetic skyrmions in the magnetic nanotrack, J. Phys. D Appl. Phys. 48 (2015) 115004.